Seismic performance assessment of a continuous highway bridge seismically isolated by lead rubber bearings

A. R. Bhuiyan, R. Alam, N. Haque

***Abstract*—This study is dedicated towards conducting seismic performance assessment of a three-span continuous highway bridge isolated by lead rubber bearing (LRB) subjected to near and far field earthquake ground motion records. A typical interior bridge pier modeled by a 2-DOF system comprising an isolation bearing (LRB) and a bridge pier is considered in the study. In the first step of the work, analytical models of the bridge pier and LRB are introduced. A visco-elasto-plastic rheology model for describing the mechanical behavior of LRB is employed, whereas a standard bilinear force-displacement relationship is employed for evaluating the nonlinear mechanical behavior of the bridge pier. In the second phase of the work, nonlinear dynamic analysis of the 2-DOF system using a standard direct time integration approach is performed to compute the seismic responses such as pier displacement, bearing displacement, bearing force and input energy. The analytical results show that the seismic responses of the system are significantly affected by the characteristics of the earthquake ground motion records.**

***Index Terms*— Visco-elasto-plastic rheology model, bilinear model, nonlinear dynamic analysis, lead rubber bearing.**

I. INTRODUCTION

Seismic isolation has been considered to be an efficient technology for providing mitigation to seismic damages for highway bridges, and has proven to be reliable and cost effective. More than 200 bridges have been designed or retrofitted in Japan and in the United States using seismic isolation in the last 20 years, and more than a thousand of bridges around the world now use this cost- effective technique for seismic protection, for example, the 29-span continuous O-Hito viaduct in Japan and the seven-span continuous steel girder Lake Saltonstall bridge in USA, etc.. In order to improve the seismic performance for both new and retrofitting applications, different forms of seismic isolation devices have widely been employed for the last few decades [1, 2]. Seismic isolation is meant to shift the natural period of a bridge structure in such a way that the dominant frequency of the earthquake ground acceleration can safely be avoided to safeguard it against the seismic damage. In addition, the inherently occupied damping property and energy dissipation mechanism prevents the bridge system from over displacement [2, 3]. Field evidence on the seismic response of isolated bridges during recent earthquakes [4], experimental research [5, 6] as well as analytical studies [7-11] have indicated that isolation devices can effectively improve the structural seismic resistance and consequently reduce the cost for repair and rehabilitation after earthquakes.

Laminated rubber bearings and sliding bearings are the two major types of seismic isolation devices, which are usually adopted for highway bridges. The sliding bearings are introduced to separate, by providing frictional sliding, the transmitting earthquake induced forces from the input earthquakes; however, this system does not encompass any re-centering capability unless a friction pendulum sliding bearing is used [12]. On the other hand, the laminated rubber bearings with high flexibility are meant to shift the natural period of bridges so as to avoid the resonance with excitations and they are usually occupied with some damping properties to prevent the isolated bridges from excessive displacement [2, 3]. Due to the capability of supporting large loads coming from superstructures while sustaining large movements with little or no maintenance requirement [13], the laminated rubber bearings have been applied more frequently in highway bridges in recent years. Three types of laminated rubber bearings are widely used for this purpose: natural rubber bearing (NRB), lead rubber bearing (LRB), and high damping rubber bearing (HDRB). Out of these, LRB, due to their relatively high damping property, are being widely used all over the world, especially in Japan and USA. LRB possesses various mechanical properties which are influenced by their compounding effect [5], nonlinear elasto-plastic behavior [14, 15] and strain-rate dependent viscosity property [15, 16]. However, the extent of inherently occupied viscosity property of LRB is revealed to be less than HDRB [15, 17, and 18].

The objective of this work is to carry out seismic performance analysis of a three-span continuous highway bridge, acted upon by near and far field earthquake ground accelerations in longitudinal direction, seismically isolated by LRB. In this regard, a nonlinear dynamic analysis is conducted using a simplified analytical model of the three-span highway bridge.

Manuscript received June 11, 2012.

A. R. Bhuiyan (corresponding author) is with the Department of Civil Engineering, Chittagong University and Technology (CUET), Chittagong-4349, Bangladesh. Phone: +880 1741 344 123; fax: +880 31 714948; E-mail: arbhuiyan@yahoo.com

R. Alam is with the Department of Civil Engineering, Chittagong University and Technology (CUET), Chittagong-4349, Bangladesh. Phone: +880 31 714948; fax: +880 31 714948; E-mail: rabiul@cuet.ac.bd

N. Haque is with the Department of Civil Engineering, Yokohama National University, Yokohama, Japan.. E-mail: naimulce@gmail.com

The bridge is simplified by a 2-DOF system comprising a typical interior bridge pier, an isolation bearing (LRB) and tributary span of the bridge deck slab. The hysteretic behavior of LRB is evaluated by a visco-elasto-plastic rheology model, whereas the hysteretic behavior of the bridge pier is modeled by a standard bilinear force-displacement relationship. Nonlinear dynamic analysis of the system using a standard direct time integration approach is performed to evaluate the seismic responses of the bridge. Finally, the variation in seismic responses of the system isolated by LRB due to two suites of earthquake ground motion records has been explored.

II. SCOPE OF THE WORK

The paper is intended to present the numerical results on seismic assessment of a 2-DOF system comprising a typical interior bridge pier, an isolation bearing (LRB) and tributary span of the bridge deck slab. In this regard, nonlinear dynamic analysis of the 2-DOF using a standard direct time integration approach is performed. A visco-elasto-plastic rheology model is used to characterize the mechanical behavior of LRB and a standard bilinear model for the bridge pier is employed in the work.

III. MODELING OF THE BRIDGE

A. *Physical model*

A typical three-span continuous highway bridge, isolated by LRB, is used in the current study shown in Fig. 1. The bridge consists of continuous reinforced concrete (RC) deck-steel girder isolated by LRB installed at bottom of the steel girder supported on RC piers. The superstructure consists of 200 mm RC slab covered by 80 mm of asphalt layer. The height of the continuous steel girder is 1800 mm. The mass of a single span bridge deck is $600\text{x}10^3$ kg and that of a pier is $240\text{x}10^3$ kg. The substructure consists of RC piers and footings supported on shallow foundation. The dimensions and material properties of the bridge deck, piers with footings are given in Table I. The geometry and material properties of LRB are presented in Fig.2 and Table II.

B. *Analytical model*

B.1 Modeling of the Bridge

The analytical model of a tributary bridge deck along with a bridge pier and an isolation bearing is shown in Fig. 1(b). The bridge model is simplified into a two-degree of freedom (2-DOF) system: one at the bridge deck level and the other at the bridge pier top level. This simplification holds true only when the bridge superstructure is assumed to be rigid in its own plane which shows no significant structural effects on the seismic performance of the bridge system when subjected to earthquake ground acceleration in longitudinal direction [7]. The mass proportional damping of the bridge pier is considered in the analysis. Equations that govern the dynamic responses of the 2-DOF system can be derived by considering the equilibrium of all forces acting on it using the d'Alermbert's principle. In this case, the internal forces are the inertia forces and the restoring forces, while the external forces are the earthquake induced forces.

Equations of motion are given as

$$m_p\ddot{u}_p(t)+F_p(u_p,t)-F_{is}(t)=-m_p\ddot{u}_g(t), \tag{1a}$$

$$m_d\ddot{u}_d(t)+F_{is}(t)=-m_d\ddot{u}_g(t), \tag{1b}$$

where m_p , m_d , u_p and u_d are the masses and displacements of pier and deck, respectively. $\ddot{u}_p$ and $\ddot{u}_d$ are the accelerations of pier and deck, respectively. $\ddot{u}_g$ is the ground acceleration. F_p is the internal restoring force of the pier to be evaluated by bilinear model. The nonlinear force-displacement relation (i.e. the bilinear model) is employed to take into account the hysteretic behavior of the bridge pier. F_{is} is the restoring force of the LRB. The restoring force of the LRB is computed using the set of Eq.(2) and becomes $F_{is}(u_p,u_d,\dot{u}_p,\dot{u}_d,\dot{\gamma}_d,t)$. The unconditionally stable Runge Kutta 4[th] order method is used in the direct time integration of the equations of motion (Eqs. (1)). For simplicity, the bottom of the pier is considered to be restrained in all directions.

B.2 Modeling of the bridge pier

The bridge pier is restricted to participate in energy absorption in the bridge system in addition to the isolation bearing. The secondary plastic behavior was expected to be lumped at bottom of the pier where plastic hinge is occurred. The plastic hinge of the pier is modeled by nonlinear spring element. Four hysteresis models for the nonlinear spring are usually used in the nonlinear dynamic analysis of a bridge structure [15]: elasto-plastic model, bilinear model, Clough degradation model, and tri-linear Takeda model. In the current study, the nonlinear spring element is modeled using the bilinear model. The ratio of the post yield stiffness to the elastic stiffness is considered to be 0.1.

B.3 Modeling of LRB

The experimental investigations conducted by several authors [5, 16, 17-19] have revealed the four different fundamental properties, which together characterize the typical overall response of laminated rubber bearings: (i) a dominating elastic ground stress response, which is characterized by large elastic strains (ii) a finite elasto-plastic response associated with relaxed equilibrium states (iii) a finite strain-rate dependent viscosity induced overstress, which is portrayed by relaxation tests, and finally (iv) a damage response within the first cycles, which induces considerable stress softening in the subsequent cycles. Considering the first three properties, a strain-rate dependent constitutive model for the LRB is developed by Bhuiyan [15] which is verified for sinusoidal excitations and subsequently implemented in professional structural

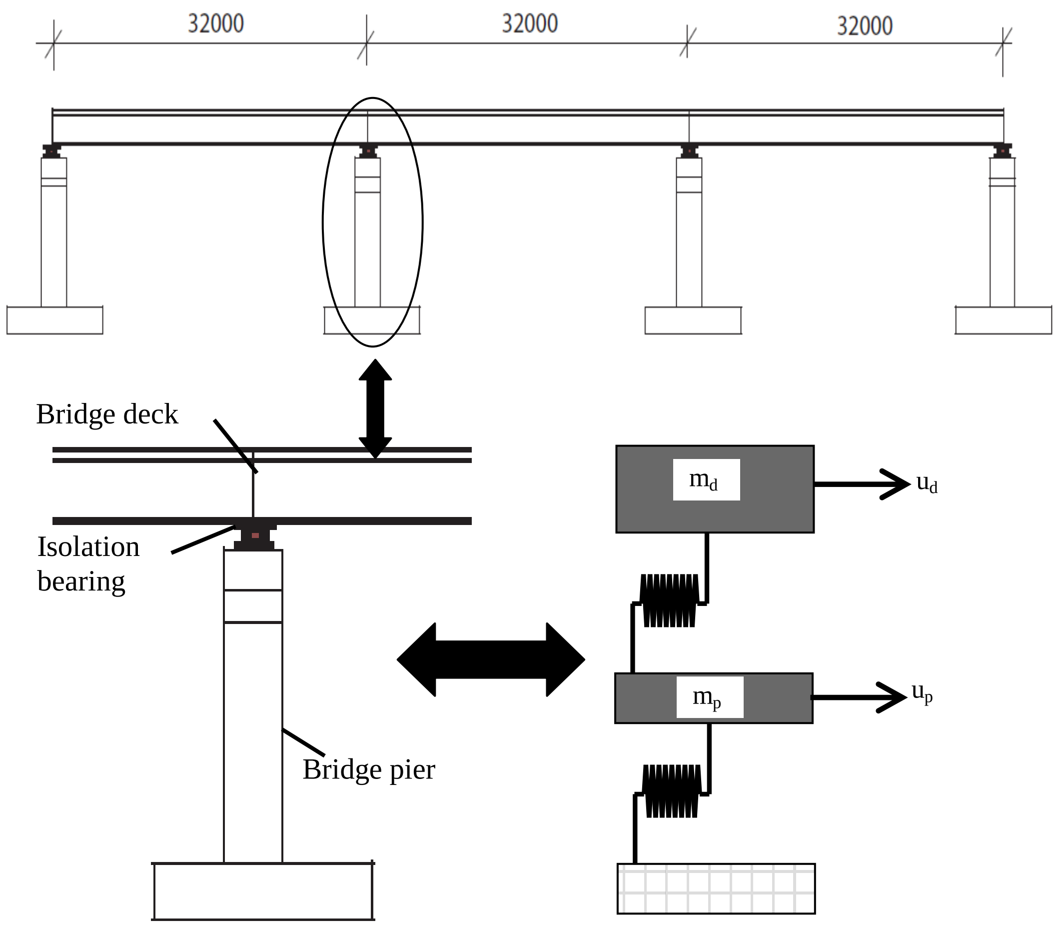

Fig. 1. Analytical modeling of the bridge pier

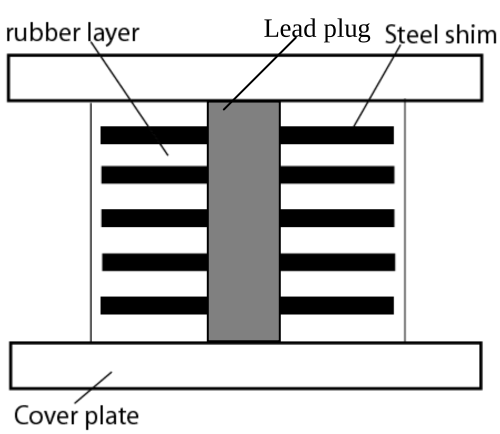

Fig.2. Typical example of lead rubber bearings (LRB)

TABLE I
GEOMETRIES AND MATERIAL PROPERTIES OF THE BRIDGE [15]

Properties	Specifications
Cross-section area of the pier cap (mm^2)	2000x12000
Cross-section area of the pier body (mm^2)	2000x9000
Height of the pier (mm)	15000
Young's modulus of elasticity of concrete (N/mm^2)	25000
Young's modulus of elasticity of steel (N/mm^2)	200000

engineering software [20] for conducting seismic performance analysis of multi-span continuous highway bridge [15, 21]. Eqs. 2(a) to 2(d) provide the explicit expressions for the average shear stress t and shear strain g of the bearings. A rigorous experimental investigation has been carried by Bhuiyan [15] to identify the parameters of the model. For more discussion, the readers are requested to refer to the earlier efforts by Bhuiyan [15] and Imai et al.[17].

$$\tau = \tau_{ep}(\gamma_a) + \tau_{ee}(\gamma) + \tau_{oe}(\gamma_c) \tag{2a}$$

$$\tau_{ep} = C_1\gamma_a \text{ with} \begin{cases} \dot{\gamma}_s \neq 0 & \text{for } \left|\tau_{ep}\right| = \tau_{cr} \\ \dot{\gamma}_s = 0 & \text{for } \left|\tau_{ep}\right| < \tau_{cr} \end{cases} \tag{2b}$$

$$\tau_{ee} = C_2\gamma + C_3|\gamma|^m \operatorname{sgn}(\gamma) \tag{2c}$$

$$\tau_{oe} = C_4\gamma_c \text{ with } \tau_{oe} = A\left|\frac{\dot{\gamma}_d}{\dot{\gamma}_o}\right|^n \operatorname{sgn}(\dot{\gamma}_d) \tag{2d}$$

where C_i ($i = 1$ to 4), τ_{cr}, m, A, n are the model parameters determined from experiments and are listed in Table III.

TABLE II
GEOMETRIES AND MATERIALS PROPERTIES OF THE ISOLATION BEARINGS

Dimension	values
	LRB
Cross-section of the bearing (mm^2)	100000
Thickness of rubber layers (mm)	200
Number of rubber layers	6
Thickness of steel layer (mm)	3.0
Nominal shear Modulus of rubber (MPa)	1.2

TABLE III
PARAMETERS FOR LRB [15]

Parameters	values
	LRB
C_1 (MPa)	4.251
C_2 (MPa)	0.710
C_3 (MPa)	0.003
C_4 (MPa)	2.351
τ_{cr} (MPa)	0.198
m	8.421
A (MPa)	0.301
n	0.253

IV. Seismic Ground Accelerations

Near fault ground motions possess some unique characteristics such as high PGV/PGA ratio and wide range of accelerations in their response spectra. They produce damaging and impulsive effects on structures which requires some special attention. Most of the seismic design guidelines are developed based on the characteristics of far-field ground motions, although the near filed earthquakes produce pulse like motion and induce high input energy on structures. Structural demands made by near-fault motions have been shown to exceed the strength, displacement and ductility capacity of structures resulting in a large increase in the inter-storey drift, base shear demand for both long and short period structures. Near field and far field ground motion differ from the distance to the rupturing fault line. According to Caltrans [22] if the structure under consideration is within 10 miles (approximately 15 km) of a fault can be classified as near-fault. Ground motions outside this range are classified as far-field motions. Recordings from recent earthquakes indicate that near field ground motion possess some features such as distinctive pulse like time histories, high peak velocities and high ground displacement. Very often the near-fault motions result in a relative increase in the vertical component of the ground motion compared to far-field motions, which can have a devastating effect depending on the strength and characteristics of the ground motion.

Two suites of four near field and four far field ground motions are used in the analysis. The near field ground motions are obtained from SAC Joint Venture Steel Project Phase 2 (http://nisee.berekely.edu/data/strong_motion/sacsteels/motion /nearfault.html). The far field ground motion histories used in the study are obtained from the FEMA P695 (ATC-63) [23] far-field ground motion set. All these ground motions have medium to strong PGA ranging from 0.44g to 0.73g. The characteristics of the earthquakes are given in Tables IV and V. Figs. 3(a) and 3(b) show the acceleration response spectra with 5 percent damping ratio of the near and far filed recorded ground motions. The response spectra of the ground motion records are well corresponding with design medium to strong earthquakes [24]. For the purpose of comparison, almost the same Richter magnitude of each the earthquake ground motion record is considered.

TABLE IV
CHARACTERISTICS OF THE FAR FIELD EARTHQUAKES

Particulars	Far Field earthquakes			
	FF-1	FF-2	FF-3	FF-4
Name	Duzce, Turkey	Loma Prieta	Loma Prieta	Superstiti on Hills
Location	Bolu	Capitola	Gilroy Array #3	Poe Road (temp)
Epicenter (km)	41.3	9.8	31.4	11.2
PGA (g)	0.73	0.45	0.56	0.44
PGV/PGA (sec)	0.77	0.77	0.64	0.82

TABLE V
CHARACTERISTICS OF THE NEAR FIELD EARTHQUAKES

Particulars	Far Field earthquakes			
	NF-1	NF-2	NF-3	NF-4
Name	Kobe	Erzincan	Loma Prieta	Northridge
Location	Takatori	Erzincan	Lex. Dam	Olive View
Epicenter (km)	4.3	2.0	6.3	6.4
PGA (g)	0.74	0.45	0.58	0.49
PGV/PGA (sec)	0.84	1.29	3.01	2.44

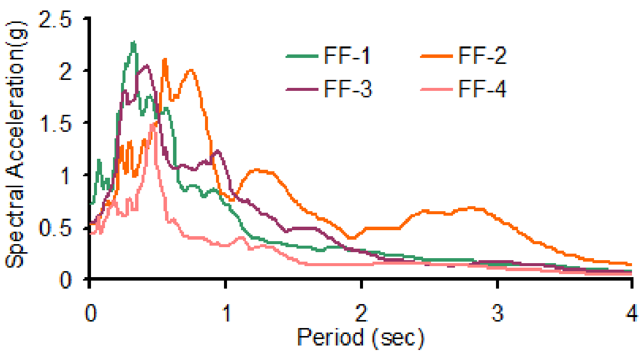

(a)

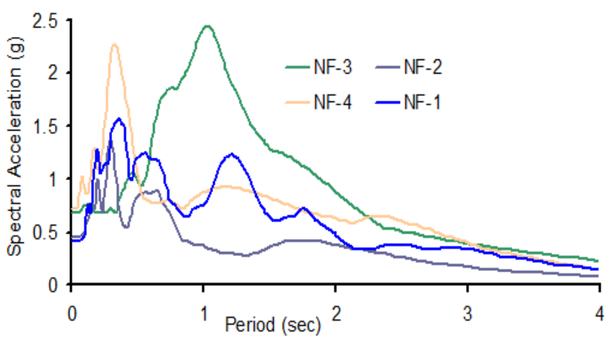

(b)

Fig.3. Spectral acceleration of the earthquake ground motion records

V. Numerical Results and Discussion

Seismic performance of the bridge system simplified by a 2-DOF system (Fig. 1) is evaluated for eight near and far field earthquake ground motion records. For simplicity, a typical interior bridge pier is considered in the seismic analysis of the bridge pier (Fig.1). An eigen-value analysis is carried out to grasp the fundamental dynamic properties of the system. The natural periods of the system isolated by LRB are found to be, respectively, 1.95 sec.

TABLE VI
Damage/limit state of bridge components

Physical phenomenon	Damage State [25]	Displacement ductility μ_d [26]	Shear strain γ (%) [10]
Cracking	Slight (DS=1)	μ_d >1.0	γ >100
Moderate cracking and spalling	Moderate (DS=2)	μ_d >1.2	γ >150
Degradation without collapse	Extensive (DS=3)	μ_d >1.76	γ >200
Failure leading to collapse	Collapse (DS=4)	μ_d >4.76	γ >250

In comparative assessment of seismic responses of the system, few standard response parameters obtained for each earthquake ground motion are addressed in the subsequent subsections: pier displacement, bearing displacement, bearing force, deck displacement and input energy. The simulation results are presented in Figs. 4 to 7. The peak seismic responses of the bridge pier system are shown in Fig.8 (a) to (d). In order to identify the damage states of the bridge components, the definitions of damage states and their corresponding damage criteria available in the literature are given in Table VI.

A. *Pier displacement*

The two factors affecting the pier displacement are energy dissipation by the bearings and the forces developed in the bearings. The pier displacement decreases with increase in energy dissipation but increases with increase in the bearing forces. Figs. 4(a) to (d) present the time histories of the pier displacement showing a significant difference in responses due near and far field earthquakes. The peak displacements of the pier are presented in Fig. 8(a) illustrating that the bridge pier produces large displacement causing, according to Table VI, extensive and collapse damage, respectively for earthquakes NF-1 and NF-3. However, the bridge pier experiences no and slight damage, respectively, for earthquakes NF-2, NF-4. From Figs. 4(a) to (d), it is noted that the bridge pier experiences no such damage due to far field earthquakes. This may be attributed to the fact that the near field earthquakes transmit higher input energy (Figs. 7(a) to (d)) to the bridge compared to far field earthquakes, which causes bigger displacement incurred by the bridge pier. In addition, the pier experiences large residual displacement shown in Figs. 4(a) to (d), particularly when acted upon by earthquakes NF-1 and NF-3.However, for the earthquakes FF-1 to FF4, the bridge pier appears no such residual displacement

B. *Bearing displacement*

The bearing displacements are obtained from relative displacements between deck and pier. Figs. 5(a) to (d) present the force-displacement response of the LRB as obtained by using the Eqs. 2(a) to (d) when subjected to earthquake ground motion records considered in the analysis. Bearing displacements directly related to its energy dissipation capacity when subjected to seismic excitations. Bearing displacement increases with the decrease of energy dissipation of the bearings as revealed from Figs. 5(a) to (d). The residual displacements of the bearings play a significant rule in selecting the suitable approach for proper repair and maintenance works of highway bridge after a seismic excitation. A residual deformation of the bearings after an earthquake makes it difficult to repair the damages on piers and elsewhere, as it is hard to place the deck to the original location. As per the damage states of the bearings defined in Table IV, the peak displacements of the isolation bearing (LRB), shown in Fig. 8(b), present no damage state in the far field earthquakes of FF-1 to FF-4; however, an extensive damage takes place in the isolation bearing (LRB), due to all the near field earthquakes except NF-2. The results shown Figs. 5(a) to (d) can be explained using the numerical results shown in Fig.7 (a) to (d). From the input energy of the bridge system as shown in Fig. 7(a) to (d), it reveals that both the NF-2 and FF-2earthquakes produce almost the same input energy after 20 mins elapsed, which has been directly reflected in the seismic responses, e.g., the bearing force-displacement response.

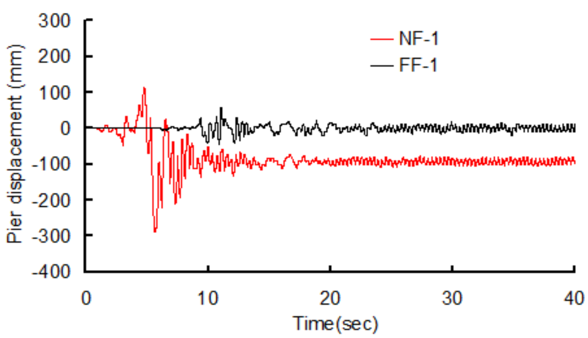

(a)

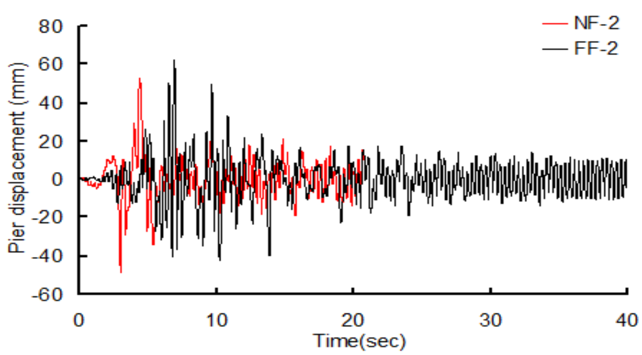

(b)

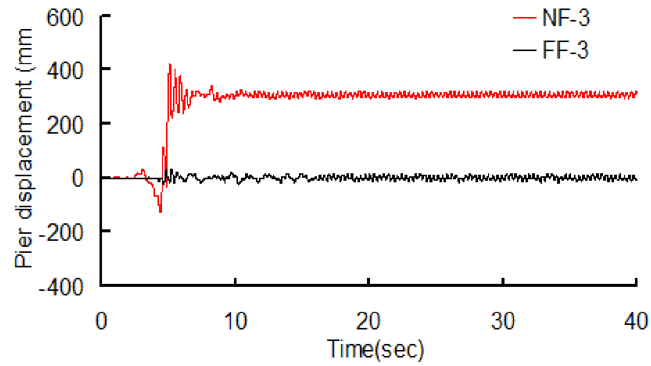

(c)

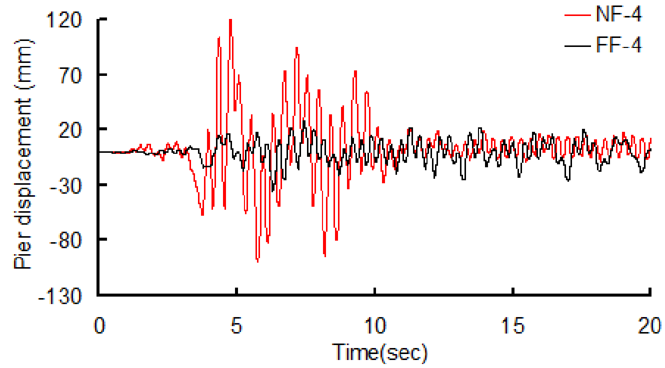

(d)

Fig.4. Pier displacement histories of the bridge system subjected to earthquake ground motion records. The legend NF and FF in each fig., respectively, represent the near and far field earthquakes.

C. Deck displacement

Figs. 6(a) to (d) present the time history of the deck displacements when subjected to earthquake ground motion records considered in the analysis. Looking at the results shown in Figs.6 (a) to (d) and Fig.8(c), the deck displacements produced by near field earthquakes appeared to be higher than that by far field earthquakes, particularly, the deck displacements due to NF-1, NF-3 and NF-4 experience three to four times higher than the corresponding far field earthquakes (FF-1, FF-3 and FF-4). The direct reflection of these results can also be observed in the case of bearing displacements. The numerical results on input energy of the bridge system shown in Figs.7 (a) to (d) illustrate the similar trend of the results.

D. Input Energy

The characteristic effect of the earthquake ground motion is analyzed by comparing the energy time histories of the bridge system for near and far field earthquakes. The input energy is defined as the total energy related to inertia forces induced by the ground motion. The mathematical formulation of the input energy is given as follows:

$$\text{Input Energy} = -m_d \int_0^{t_0} \ddot{u}_g . \dot{u}_d \, dt - m_p \int_0^{t_0} \ddot{u}_g . \dot{u}_p \, dt \; , \qquad (3)$$

where t_0 is the time duration of the given earthquake ground motion and the other variables are defined in Sub-section B.1.

Figs. 7(a) to (d) show the variation of input energy of the bridge pier system due near and far field earthquakes. From each fig. it is revealed that input energy of the system due to near filed earthquakes is several times bigger than the far filed earthquakes except the earthquake NF-2 and FF-2. The direct reflection of this phenomenon is observed in each seismic response of the system shown in Figs. 4 to 8.

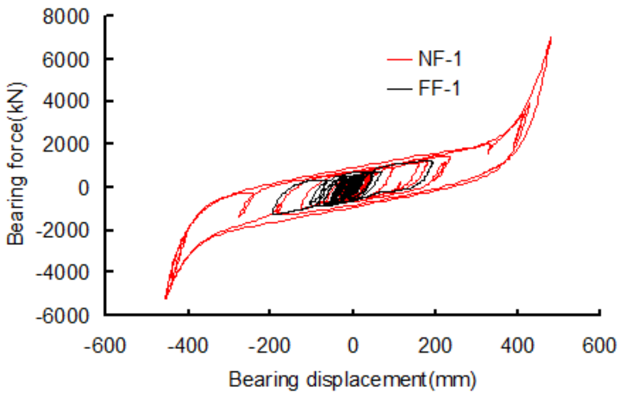

(a)

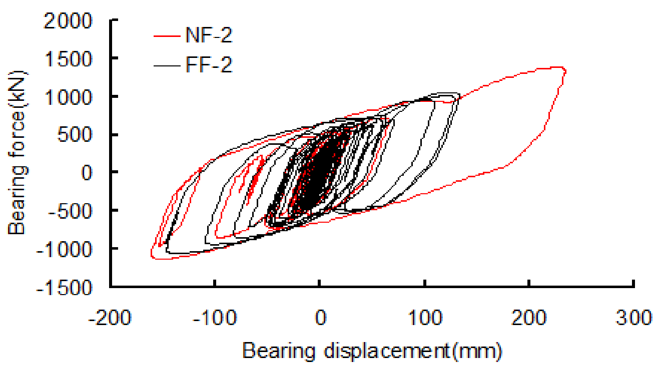

(b)

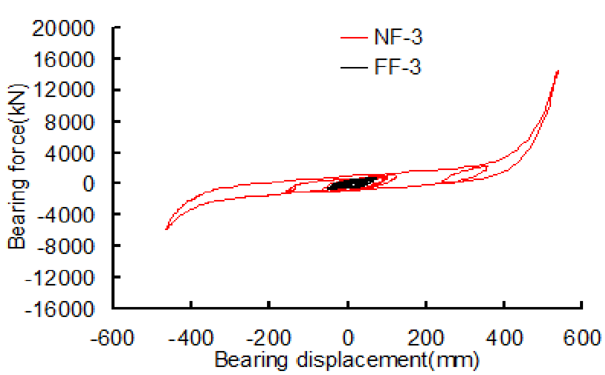

(c)

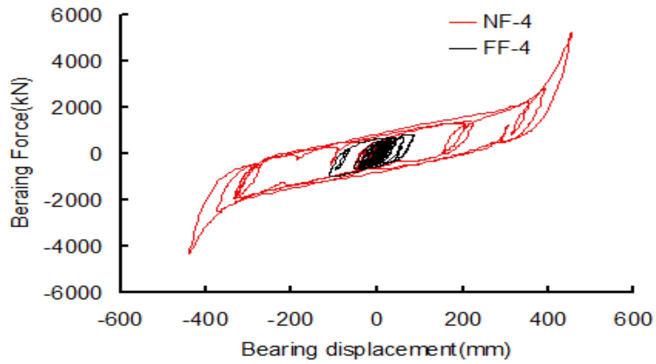

(d)

Fig.5. Bearing force-displacement responses of the bridge system subjected to earthquake ground motion records. The legend NF and FF in each fig., respectively, represent the near and far field earthquakes.

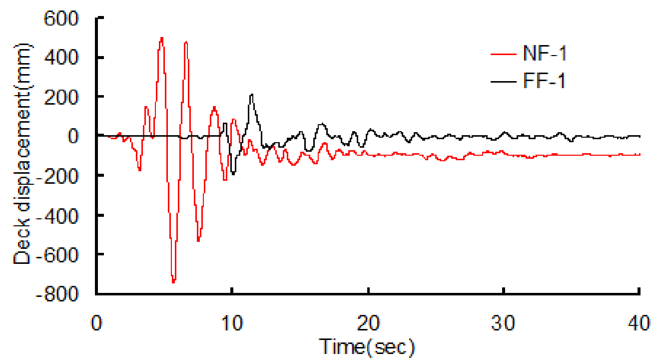

(a)

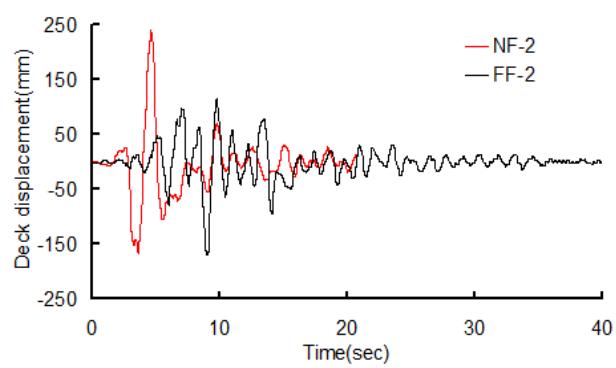

(b)

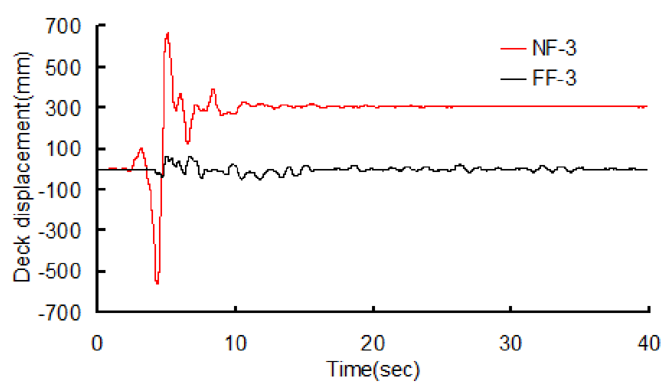

(c)

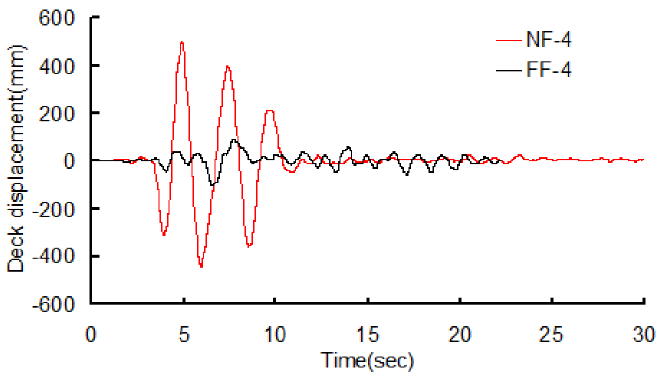

(d)

Fig.6. Deck displacement histories of the bridge system subjected to earthquake ground motion records. The legend NF and FF in each fig., respectively, represent the near and far field earthquakes.

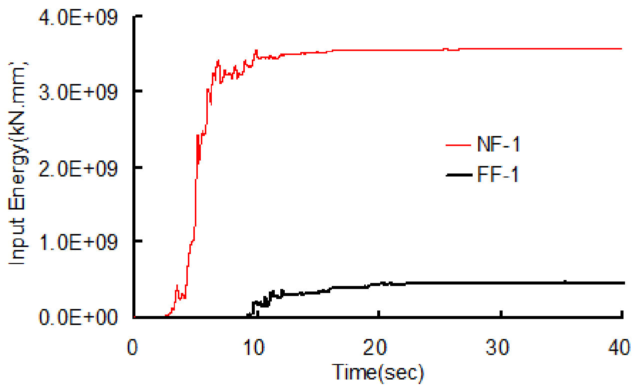

(a)

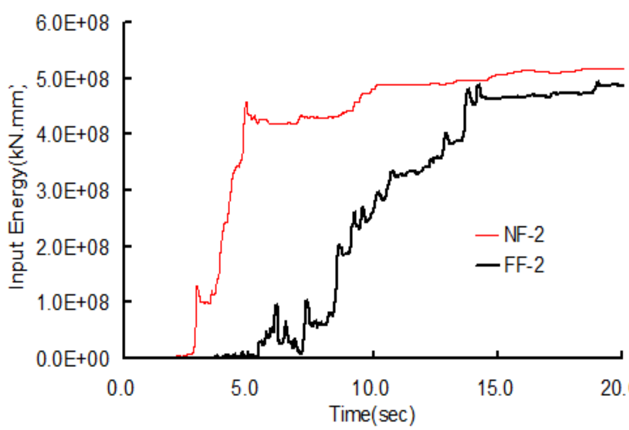

(b)

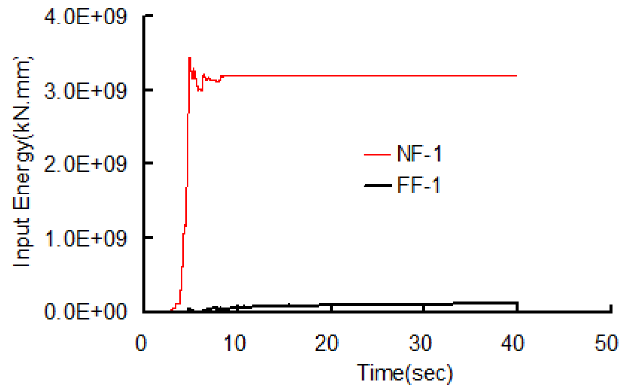

(c)

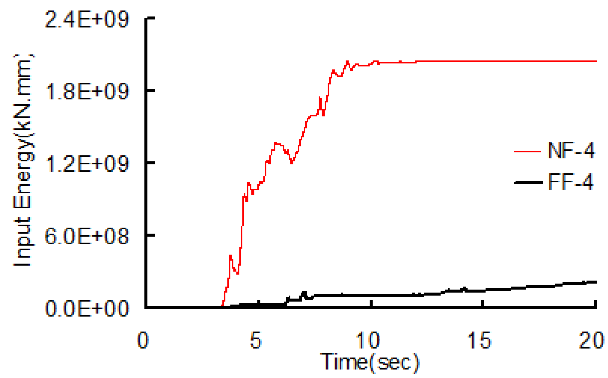

(d)

Fig.7. Input energy histories of the bridge system subjected to earthquake ground motion records. The legend NF and FF in each fig., respectively, represent the near and far field earthquakes.

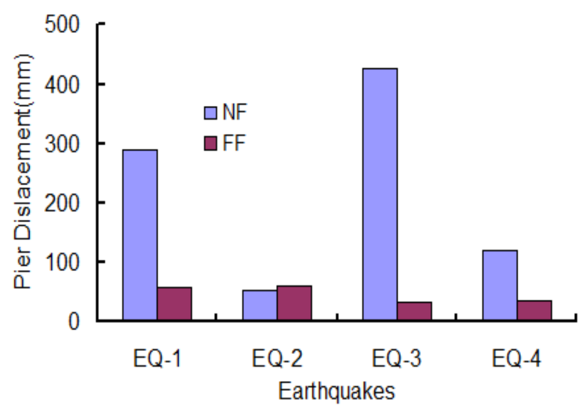

(a)

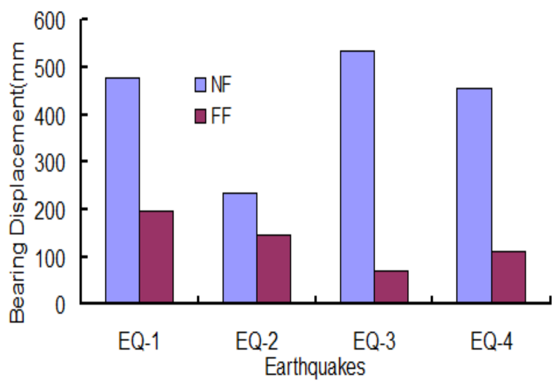

(b)

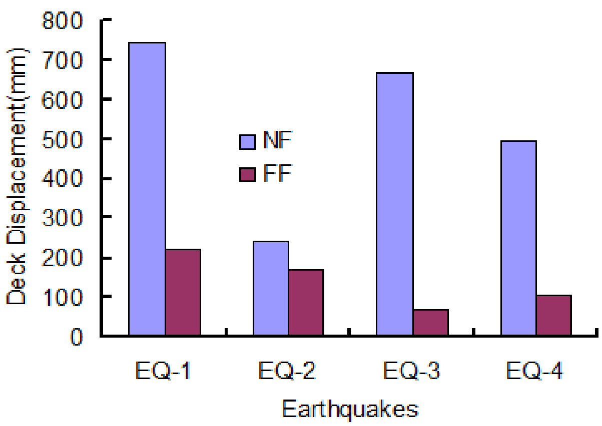

(c)

Fig.8. Comparison of the peak responses of the bridge system subjected to earthquake ground motion records. The legend NF and FF in each fig., respectively, represent the near fault and far field earthquakes.

VI. Concluding Remarks

This study presents the seismic performance assessment of a bridge system isolated by lead rubber (LRB). The bridge is analyzed for two suites near and far field earthquake ground acceleration records. The nonlinearity of the bridge pier is considered by employing a bilinear force-displacement relationship, whereas an visco-elasto-plastic rheology model is employed to evaluate the mechanical behavior of LRB under seismic excitations.

The numerical results have revealed that the seismic responses of the bridge system are significantly affected by the characteristics of the earthquakes ground motion records. For example, the input energy transmitted to the bridge system due to near field earthquakes is several times higher than the far filed earthquakes even though the earthquake records with almost the same magnitudes have been considered in each case. The consequence effect of this phenomenon has been reflected in seismic responses considered in the current study. From the numerical analysis conducted in the current study it can be concluded that not only the magnitude but the other characteristics of earthquake ground motions also have significant effect on the seismic responses of the bridge which should be carefully considered in the design phase of bridge system.

In the current study, only one interior bridge pier is considered; however, a more rigorous modeling of the bridge system is expected for an elaborate numerical investigation since the seismic responses of such a simplified sub-assemblage would be different if an exterior pier is considered instead, or the total assembly of the bridge is considered. This is likely to change the dynamics of the response of the entire bridge structure. This can be dealt with in future work. It should be also noted that the selection of the type and modeling approach of isolation bearings may have a remarkable effect on the seismic performance evaluation of highway bridges, which should be carefully considered in the analysis and design steps of any bridge project.

Acknowledgment

The authors gratefully acknowledge to the University Grants Commission, Bangladesh for the financial assistance provided to carry out this research work at Chittagong University of Engineering and Technology (CUET).

References

[1] F. Naeim and J. Kelly , “Design of seismic isolated structures”, 1st edition, John Wiley and Sons, New York, 1996

[2] J. M. Kelly, “Earthquake resistant design with rubber”, 2nd edition, Springer-Verlag Berlin Heidelberg, New York, 1997

[3] R.I. Skinner, W. H. Robinson, G.H. McVerry, “An introduction to seismic isolation”, DSIR Physical Science, Wellington, New Zealand, 1993

[4] M. T. A. Chaudhary, M. Abe and Y. Fujino “Performance evaluation of base- isolated Yama-agé bridge with high damping rubber bearings using recorded seismic data”, *Engineering Structures* vol. 23, pp. 902-910, 2001

[5] J. S. Hwang, J. D. Wu, T. Pan, G. Yang, “A mathematical hysteretic model for elastomeric isolation bearings”, *Earthquake Engineering and Structural Dynamics*, vol. 31, pp. 771-789, 2002

[6] M. Kikuchi, I. D. Aiken, “An analytical hysteresis model for elastomeric seismic isolation bearings” *Earthquake Engineering and Structural Dynamics*, vol. 26, pp. 215-231, 1997.

[7] Ghobarah, A., Ali, H. M. (1988), “Seismic performance of highway bridges”, Engineering Structures, 10, 157-166.

[8] O. E. Ozbulut, S. Hurlebaus “Optimal design of superelastic-friction base isolators for seismic protection of highway bridges against near-field earthquakes”, *Earthquake Engineering and Structural Dynamics*, vol. 40, pp. 273–291, 2011

[9] O. E. Ozbulut, S. Hurlebaus “Seismic assessment of bridge structures isolated by a shape memory alloy/rubber-based isolation system”, *Smart Materials and Structures*, vol. 20, 2011

[10] J. Zhang, Y. Huo, “Evaluating effectiveness and optimum design of isolation devices for highway bridges using the fragility function method”, *Engineering Structures*, vol. 31, pp. 1648-1660, 2009.

[11] K. Wilde, P. Gardoni, Y. Fujino, “Base isolation system with shape memory alloy device for elevated highway bridges”, *Engineering structures*, vol. 22, pp. 222–229, 2000.

[12] Y.P. Wang, L. Chung and H.L. Wei, “Seismic response analysis of bridges isolated with friction pendulum bearings”, Earthquake Engineering and Structural Dynamics, vol. 27, pp. 1069-1093, 1998

[13] H.M. Ali, A.M. Abdel-Ghaffar, “Modelling of rubber and lead passive-control bearings for seismic analysis”, *Journal of Structural Engineering*, vol. 121, pp. 1134-1144, 1995

[14] M. Abe, J. Yoshida, Y. Fujino, "Multiaxial behaviours of laminated rubber bearings and their modeling I: Experimental study", *ASCE Journal of Structural Engineering*, vol. 130, pp. 1119-1132, 2004.

[15] A.R. Bhuiyan, "Rheology modeling of laminated rubber bearings", PhD dissertation. Graduate School of Science and Engineering, Saitama University, Japan, 2009

[16] A. R. Bhuiyan, Y. Okui, H. Mitamura, and T. Imai, "A Rheology model of high damping rubber bearings for seismic analysis: identification of nonlinear viscosity", *Int. Journal of Solids and Structures*, vol. 46, pp.1778-1792, 2009.

[17] T., Imai, A.R. Bhuiyan, M. K. Razzaq, Y. Okui and H. Mitamura, "Experimental studies of rate-dependent mechanical behaviour of laminated rubber bearings", *Joint Conference Proceedings, 7th International Conference on Urban Earthquake Engineering (7CUEE) & 5th International Conference on Earthquake Engineering (5ICEE)*, March 3-5, 2010, Tokyo Institute of Technology, Tokyo, Japan.

[18] W.H. Robinson, "Lead rubber hysteresis bearings suitable for protecting structures during earthquakes", *Earthquake Engineering and Structural Dynamics*, vol. 10, pp. 593-604, 1982

[19] C. Miehe, and J. Keck, "Superimposed finite elastic-viscoplastic-plasto-elastic stress response with damage in filled rubbery polymers:Experiments, modeling and algorithmic implementation", *Journal of Mechanics and Physics of Solids*, vol. 48, pp. 323-365, 2000

[20] Resp-T, "User's Manual for Windows, Version 5", 2006

[21] M. K., Razzaq, A.R. Bhuiyan, Y. Okui, H. Mitamura and T. Imai, " Effect of rubber bearings modelling on seismic response of base", *Joint Conference Proceedings, 7th International Conference on Urban Earthquake Engineering (7CUEE) & 5th International Conference on Earthquake Engineering (5ICEE)*, March 3-5, 2010, Tokyo Institute of Technology, Tokyo, Japan.

[22] California Department of Transportation , "Seismic Design Criteria (CALTANS)", Sacramento, CA., 2004

[23] Federal Emergency Management Agency (FEMA P695), (ATC-63) Applied Technology Council (ATC), Redwood City, Calif.,2009

[24] Japan Road Association (JRA) "Specifications for highway bridges-Part V: Seismic design", Tokyo, Japan, 2002.

[25] Federal Emergency Management Agency (FEMA) "HAZUS-MH software," Washington DC., 2003

[26] H. Hwang, J. B. Liu, Y. H. Chiu, "Seismic fragility analysis of highway bridges" *MAEC report: project MAEC RR-4. Urbana: Mid-America Earthquake Center*, 2001